Wavelength dependence of prepulse laser beams on EUV emission from CO_2 reheated Sn plasma

J. R. Freeman[a], S. S. Harilal[a], T. Sizyuk[a], A. Hassanein[a], and B. Rice[b]

[a]Center for Materials Under Extreme Environment, School of Nuclear Engineering
Purdue University, West Lafayette, IN 47907, USA;
[b]SEMATECH Inc., Albany, NY 12203, USA

ABSTRACT

Extreme ultraviolet (EUV) emission from laser-produced plasmas (LPP) centered at 13.5 nm is considered a leading candidate for the light source in future lithography systems. Tin is currently the best material for generating this EUV emission since it emits strongly within the 13.5 nm region due to its various ionic states (Sn^{8+}- Sn^{14+}). Highly efficient and low-debris LPPs are a pre-requisite for their use as light sources for EUV lithography. Tin plasmas generate debris that can damage collection optics over time. Techniques to mitigate debris are needed to extend the lifetime of these components and the system. Optimization of plasma conditions is necessary for increasing EUV emission and enhancing conversion efficiency (CE). Improving the source CE is necessary in order to reduce the cost of ownership and hence, develop a commercially viable lithography system for the semiconductor industry. One method to accomplish this is to reheat pre-formed plasma with a laser pulse to enhance EUV emission. This enhancement is achieved by controlling those plasma conditions necessary for optimizing EUV emission. We investigated the role of prepulse laser wavelength on prepulse plume formation and EUV in-band signal enhancement. A 6 ns Nd:YAG laser operating at 1064 nm and 266 nm was used for generating the prepulse plume. The expanding plume was then reheated by a 35 ns CO_2 laser operating at 10.6 μm. The role of prepulse wavelength and energy on EUV conversion efficiency is discussed.

Keywords: EUV lithography, Laser-produced plasma, Extreme ultraviolet spectroscopy, Plasma sources, Conversion efficiency, Spectral emission, Ionic emission, Plasma diagnostics

1. INTRODUCTION

EUV light centered at 13.5 nm is currently the leading light source for the next generation of lithography and semiconductor manufacturing. The 13.5 nm light has been chosen because of the availability of Mo/Si multilayer mirrors exhibiting 70% reflectivity at 13.5 nm within 2% bandwidth.[1] Before commercialization of such a system can occur, an efficient and low-debris source of 13.5 nm light must be realized. Li, Xe, and Sn have all be considered as sources of 13.5 nm light.[2] Because of its broad emission centered at 13.5 nm, Sn has become the main material of interest for EUV lithography applications. Its broad emission is referred to as the Sn unresolved transition array (UTA) and is caused by Sn^{8+}- Sn^{14+} ion transitions.

The two competing methods for generating 13.5 nm light are discharge-produced plasma (DPP) and laser-produced plasma (LPP). Considerable efforts have been made to improve the efficiency and to understand the plasma dynamics from these sources.[3-5] LPP source research has taken precedence over DPP sources due to its improved scalability for high volume manufacturing scanners.[3, 6] LPP experiments using Sn have produced high conversion efficiencies (CE) of 2-5%[4, 7, 8] while modeling studies have predicted up to 7%.[9] Nd:YAG lasers have been shown to produce high CE,[10] but in 2005, Tanaka *et al.*[11] demonstrated the advantages of using a CO_2 laser for generating higher CE. The CO_2 LPP, despite producing more energetic ions, has also been shown to produce one-fourth the particle emission and debris accumulation than that produced by a Nd:YAG LPP at the same laser energy.[12-14] The differences between Nd:YAG and CO_2 LPP are attributed to the order of magnitude difference in laser wavelength between the two. As the critical density of the plasma is related to laser wavelength by $n_{ec} \propto \lambda^{-2}$, the plasma heating mechanisms differ.[7]

Extreme Ultraviolet (EUV) Lithography III, edited by Patrick P. Naulleau,
Obert R. Wood II, Proc. of SPIE Vol. 8322, 83220H · © 2012 SPIE
CCC code: 0277-786X/12/$18 · doi: 10.1117/12.916161

Methods used to improve EUV emission and cleanness of the lithography system are accomplished by altering target geometry, varying laser parameters, and implementing debris mitigation techniques. Mass-limited targets[9, 15-18] have been used to lower plasma density and limit self-absorption of EUV light while also producing less Sn debris. Laser parameters including wavelength,[7] intensity,[19] and spot size[20] have also been studied to determine their effect on EUV emission and debris generation.

Double pulse laser irradiation schemes have been demonstrated to increase EUV and x-ray emission from plasma sources,[5, 15, 21-23] with modeling[9] showing that refinement of parameters can increase this further. In a double pulse scheme, a low energy prepulse is used to ablate the target, creating a low-density prepulse plume that is then reheated by the pumping pulse, generating increased emission. In this article we compare the effect that different prepulse wavelengths plays in generating increased EUV emission. This is done by varying the delay between prepulse and pumping pulse and studying the resulting EUV emission spectra and Sn ion profiles from the plasma.

2. EXPERIMENTAL SETUP

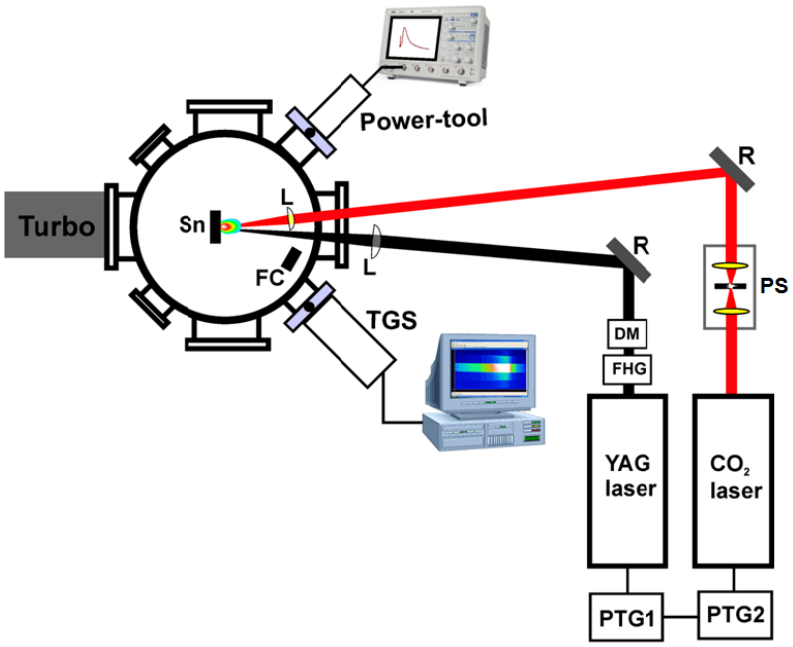

Figure 1. Schematic illustration of the experimental setup (PTG, programmable timing generator; FHG, fourth harmonic generator; DM, dichroic mirror; PS, plasma shutter; R, reflective optics; L, lens; FC, Faraday cup; TGS, transmission grating spectrograph). Nd:YAG laser generates a prepulse plume that is reheated by the CO_2 laser at a set time delay. Triggering of both lasers is performed using timing generators.

A schematic illustration of the experimental setup employed in our Center for Materials Under eXtreme Environment (CMUXE) is shown in Figure 1. The experiment was conducted using a planar Sn target in a vacuum chamber evacuated to a pressure of ~10^{-6} Torr using a turbo pump. A 6 ns full width half maximum (FWHM) Nd:YAG laser operating at its fundamental (1064 nm) or fourth (266 nm) harmonic was used as a prepulse to generate a prepulse plume from the target. This plume serves as a low-density Sn target. After a predetermined delay, the plume is reheated by a 35 ns FWHM transversely excited atmospheric (TEA) CO_2 laser (10.6 μm) to generate EUV emission. A plasma shutter was used to eliminate the long nitrogen tail of the CO_2 laser pulse. This method eliminates the long tail of the traditional CO_2 laser pulse.[24] Two timing generators were used to control the timing of the two lasers. One timing generator was used to trigger the flash lamps of the Nd:YAG laser, thereby minimizing thermal lensing effects, and the second timing generator was used to trigger the lasers with a set delay between both shots. All experiments were performed in a single-shot manner. Both lasers were aligned to interact with the target at an angle of 5° off-normal. Spot sizes used in this experiment were 100 μm and 225 μm for Nd:YAG and CO_2 lasers, respectively. The Sn target was repositioned to a fresh target spot for each laser shot.

The ion dynamics of the Sn plasma were collected using a FC positioned 19.8 cm from the target and at an angle of 25° off-normal and biased with a -31 V DC voltage. This data was used to compare time-of-flight (TOF) data of ions and was analyzed to provide the energy spectra of the ions. In-band EUV energy was collected using an absolutely-calibrated EUV Power Tool at an angle of 45° with respect to the target. The Power Tool consists of two 150 nm Zr filters, a Mo/Si mirror, and an EUV photodiode that collects 13.5 nm light within a 2% bandwidth. The EUV CE was calculated using the EUV energy over a 2π sr solid angle. Signals from the FC and EUV Power Tool were collected and saved using a 1 GHz digital oscilloscope. EUV light spectra were obtaining using an EUV transmission grating spectrograph. The spectrograph uses a 10,000 lines/mm silicon nitride grating and is connected to a back-illuminated EUV sensitive charge coupled device (CCD).

3. RESULTS AND DISCUSSION

Our previous studies[4, 8] have shown that highest EUV CE from the CO_2 laser can be achieved using a laser intensity of 6×10^9 W/cm^2 with a spot size of 225 μm. Therefore, this was approximately the laser intensity used throughout the experiments. At this laser intensity, the peak density of the CO_2 LPP has been measured[4] to be 5.5×10^{19}/cm^3. This is higher than the critical density of a CO_2 LPP (9.8×10^{18}/cm^3). Once critical plasma density is reached, the laser pulse is blocked by the plasma and can no longer interact with the target. At this stage in irradiation, laser energy is then deposited onto the coronal region of the plasma. EUV photons produced in this coronal region are able to escape the plasma without being absorbed by the plasma itself, whereas those produced within the plasma closer to the target surface can end up reabsorbed by the plasma itself. In the case of the Nd:YAG LPP, the critical plasma density is two orders of magnitude higher at fundamental (9.8×10^{20}/cm^3) and over three orders higher at fourth harmonic (1.6×10^{22}/cm^3) wavelengths than that of the CO_2 LPP. Because of the higher critical density, laser energy is deposited mainly near the target surface and EUV photons are more likely to be absorbed as they travel through the dense plasma. This is the cause of lower CE for Nd:YAG LPP than for CO_2 LPP having the same power density.

The critical density of the LPP must be considered when determining which laser should serve as the prepulse and which as the pumping pulse. In our previous report[23] we explained that due to critical density differences of two orders of magnitude, if the CO_2 laser served as the prepulse, a Nd:YAG pumping pulse would penetrate through the pre-plasma and interact with the target, rather than the lower-density pre-plasma, and a similar scenario to the single-shot Nd:YAG LPP would occur. This would result in dense plasma exhibiting strong self-absorption of EUV photons and a low CE. On the other hand, if the Nd:YAG laser served as the prepulse, the dense pre-plasma would be opaque to the CO_2 pumping pulse and CO_2 laser energy would instead be deposited onto the coronal region of the pre-plasma. EUV photons generated in the coronal region are less likely to be reabsorbed by the plasma and have a higher escape probability, resulting in a higher CE. This scenario provides higher CE.

In our previous study[23] we observed an increase in CE of about 40% by using a 1064 nm Nd:YAG prepulse and 10.6 μm CO_2 pumping pulse. It was found that the increase in CE was dependent on the delay between prepulse and pumping pulse and prepulse spot size. The delay between pulses allows for formation of the prepulse plume and its expansion to the spot size of the pumping pulse in order to achieve proper coupling between plume and pumping pulse.[5] By comparing EUV spectra it was found that the increase in CE was due to an increase in intensity of the EUV light as well as a broadening of the Sn UTA. However, it was found by comparing Sn ion TOF profiles that only a small portion of the pumping pulse was absorbed by the plume. It was hypothesized that by increasing plume density, coupling between prepulse plume and pumping pulse could be improved and further increases in EUV emission may be possible.

In this study we examined the effects of prepulse wavelength on EUV emission for generating a higher-density prepulse plume and improving coupling between the plume and pumping pulse. A 10.6 μm CO_2 laser with pulse energy of 90 mJ and power density of 6.5×10^9 W/cm^2 was used throughout the experiment as the pumping pulse. The Nd:YAG laser operating at its fundamental (1064 nm) and fourth harmonic (266 nm) wavelengths with an energy of 15 mJ and power density of 3.2×10^{10} W/cm^2 was used as the prepulse. Spectra and TOF data were taken for the individual prepulses and pumping pulse for comparisons. For each prepulse wavelength, a delay range scan was performed to find the delay between prepulse and pumping pulse where EUV emission was maximum. At this peak delay time, EUV emission spectra and TOF data were recorded. These were compared against the data collected for the individual prepulses and pumping pulse shots to determine the cause of increased EUV emission and to identify any differences between using fundamental and fourth harmonic Nd:YAG radiation for the prepulse.

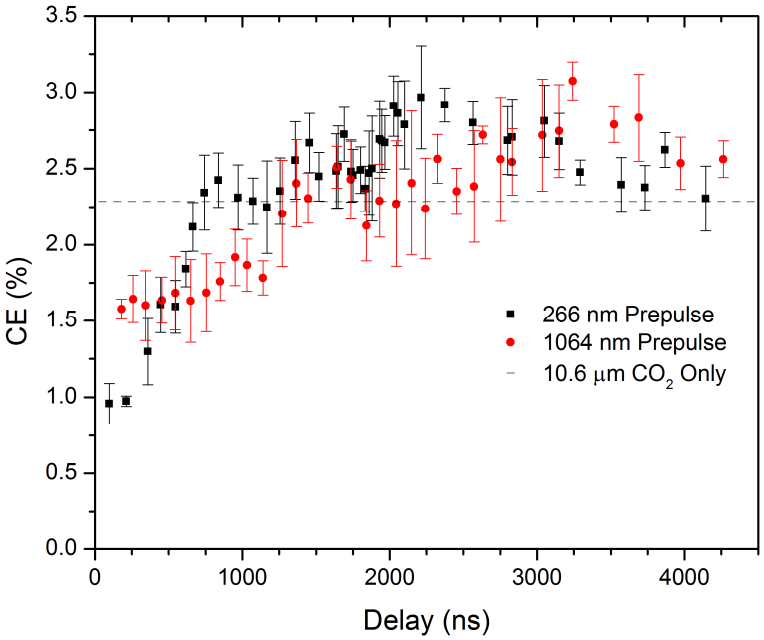

Figure 2. Dependence of CE on delay time between prepulse and pumping pulse for 266 nm and 1064 nm prepulsed shots. CE from the pumping pulse alone is 2.3%.

Figure 2 shows the delay range scan for 266 nm and 1064 nm prepulsed shots and the resulting CE of EUV. Spatial alignment of the pumping pulse with respect to the prepulse plume is crucial. Minute changes in alignment as well as focal position of the laser pulse can affect CE and greatly affect delay times[23] due to plume expansion and coupling with the pumping pulse. The position of the detector and solid angle used to collect EUV emission can also have an effect on estimating the overall CE. As can be seen in the figure, the peak delay for the 266 nm prepulse occurs around 2.25 μs at 3.0%. With a pumping pulse CE of 2.3%, this represents 30% increase in EUV emission. The peak CE for the 1064 nm prepulse is also 3.0%, but requires a longer delay, around 3.4 μs.

While the 1064 nm prepulse requires a longer delay to reach peak CE, both sets of data display similar trends. For short delays between prepulse and pumping pulse, CE is very low, but begins to increase with increasing delay. A reduction in CE is observed at early inter-pulse delay times (<750 ns). The denser 266 nm prepulse plume shows a greater drop in CE than the less-dense 1064 nm plume. After the initial low CE at short delays, CE of both data sets increases gradually with increasing delay before reaching its peak. At the peak, the prepulse plume is dense enough to absorb the pumping pulse radiation, but is not dense enough to absorb the EUV photons that have been created within the plume and from interaction with the target surface. After their respective CE peaks, both sets of data gradually decrease, as the plume is dispersed and the pumping pulse interacts mainly with the target surface.

The optimum inter-pulse delay for both prepulse wavelengths are >1 μs. At the peak delay time, the prepulse plume can be expected to contain mostly neutral Sn atoms and small clusters in the cold plasma. Ultimately, the optimum delay time depends on many factors to best couple the prepulse plasma with the main pumping pulse to create ideal temperature and density conditions to produce, as well as to transmit, the most EUV photons. Therefore, other prepulse and main pulse combinations can still exist to produce even higher CE.

Figure 3 shows time-integrated spectral comparisons between the prepulsed shot spectra at their respective peak delays and those obtained for the individual prepulse and pumping pulse. As can be seen in the figure, the use of a prepulse both increases the spectral intensity and broadens the UTA for both 266 nm and 1064 nm prepulse spectra. This is the cause of the increased CE identified in Figure 2. From the spectra, CE can be understood as the area enclosed by the spectra within a 2% bandwidth centered at 13.5 nm.

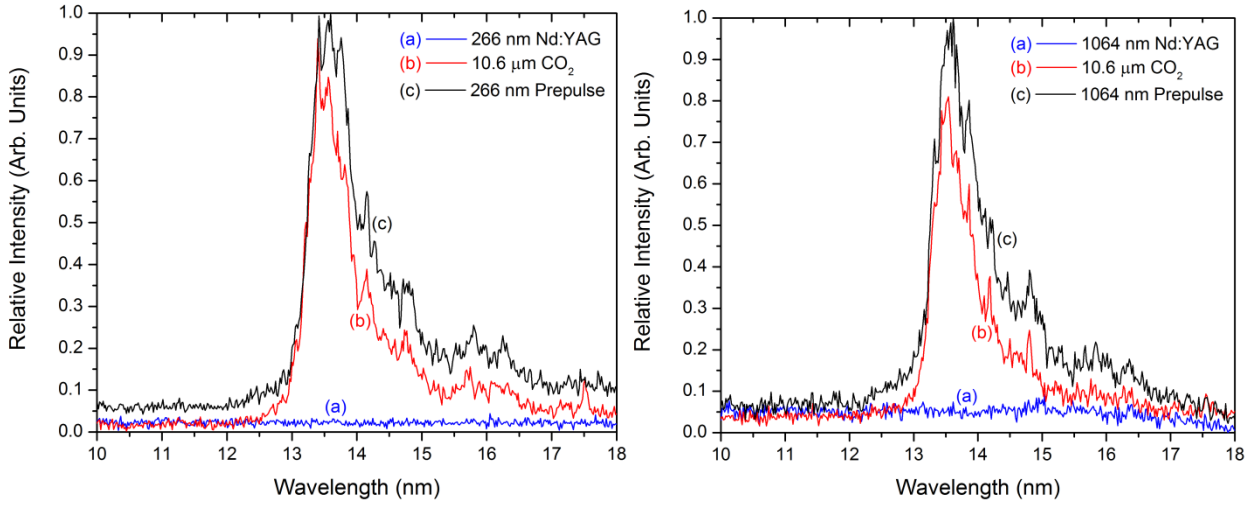

Figure 3. EUV spectral data obtained using a transmission grating spectrograph and EUV sensitive camera for 266 nm (left) and 1064 nm (right) prepulses at their respective peak delays compared to the individual pumping pulse and prepulse alone. Both prepulses resulted in increased spectral intensity and broadening of the UTA.

The individual 266 nm and 1064 nm Nd:YAG spectra produced negligible EUV emission for the laser intensity used. From this it can be concluded that the increase in intensity by using a prepulse is due to the interaction of the pumping pulse with the prepulse plume and not from the prepulse's own emission. The broadening of the UTA indicates that additional ionic states of Sn were excited when reheating the plume. As the broadening occurs mainly on the higher-wavelength side of the UTA, it is the lower-energy ionic states are excited. While broadening within the 13.5 nm in-band region is desirable, out-of-band (OoB) broadening worsens spectral purity and should be avoided, as it causes increased heat load to collection optics. From Figure 3, a definitive difference between the EUV spectra generated using a 266 nm and 1064 nm prepulse cannot be discerned. Both spectra indicate a similar increase in intensity and a broadening of the higher-wavelength, lower-energy side of the UTA, producing comparable CE results.

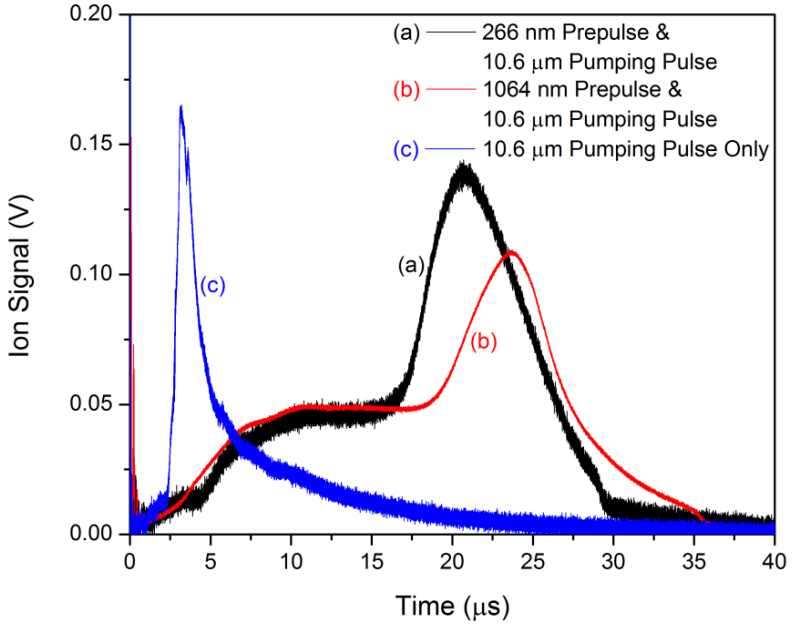

Figure 4. TOF comparison between the individual pumping pulse and the pumping pulse shots fired after a prepulse at their respective peak delays. Zero time corresponds to the start of the CO_2 laser pumping pulse. By using a prepulse before the pumping pulse, ions generated by the pumping pulse are slowed significantly.

Figure 4 shows the TOF comparison between the individual pumping pulse and the prepulsed shots at their respective peak delays of approximately 2.25 μs and 3.4 μs after the prepulse for 266 nm and 1064 nm prepulses, respectively. Both sets of prepulse data display two significant features. The first feature is a slow rise in the signal that levels off. This part of the signal corresponds to ions that were excited within the prepulse plume by the pumping pulse. The second feature is the peak at about 21 μs for the 266 nm prepulse and around 24 μs for the 1064 nm prepulse. This peak corresponds to the ions excited by the pumping pulse interacting with the target.

For EUV lithography systems, Figure 4 provides important insight. Highly energetic ions and other forms of debris from Sn plasma are a major consideration in the design of a lithography system. These ions cause significant sputtering damage and interlayer mixing of multilayer collection optics. Methods to reduce debris and lower kinetic energies of debris will be necessary for commercialized systems. This figure shows a significant slowing-down of Sn ions from the pumping pulse. The ion flux of the individual pumping pulse peaks at about 3.1 μs, while the flux peaks in the prepulse data occur 21 μs and 24 μs after the pumping pulse for 266 nm and 1064 nm prepulses, respectively. As kinetic energy is proportional to t^{-2}, this slowing down of Sn ions represents a substantial decrease of the most probable ion energies. The ratio of these ion kinetic energies can be expressed as 1 : 0.022 : 0.017 (pumping pulse: 266 nm prepulse: 1064 nm prepulse). This is a reduction in most probable kinetic energy of nearly two orders of magnitude, greatly mitigating the sputtering and interlayer mixing damage of optics by these Sn ions. It is important to note that total ion fluence, albeit consisting of lower energy ions, is roughly 2.65 times greater for the prepulsed plasmas than for the individual pumping pulse plasma. This is due to the ions produced by the prepulse and those in the prepulse plume that are reheated by the pumping pulse. Despite their higher fluences, the less energetic ions found in prepulsed plasmas are much easier to mitigate by use of electric and magnetic field techniques.

4. CONCLUSION

In this report a detailed study of the effect of different prepulse wavelengths for EUV lithography systems was conducted. Wavelengths of 266 nm and 1064 nm prepulses from a Nd:YAG laser were used to generate a plasma plume from a planar Sn target. The plume was then reheated by a 10.6 μm CO_2 laser pumping pulse to generate EUV emission. The delay time between prepulse and pumping pulse was varied for each prepulse wavelength to identify the delay in which peak CE was realized. It was found that both prepulse wavelengths produced similar EUV emission improvements of 30%, albeit at different delay times due to differing plume expansion velocities. Trends in the delay range data were also similar between both prepulse wavelengths, but were more drastic for the 266 nm prepulse. EUV emission spectra were then analyzed to determine the cause of the increased CE. At their respective peak delays, spectra from both prepulse wavelengths showed an increase in emission intensity as well as a broadening of the Sn UTA on the lower-energy, higher-wavelength side. A definitive difference from spectra between the two prepulse wavelengths cannot be discerned. TOF profiles of Sn ions indicated a substantial slowing down and hence, reduction in kinetic energy by nearly two orders of magnitude for both prepulse wavelengths when compared to that of the individual pumping pulse. While total ion fluence was greater with the implementation of a prepulse, the substantial decreases in kinetic energy provides for easier debris mitigation through the use of electric and magnetic fields. This can lower the damage to collection optics by energetic ions.

With this information it appears there is no substantial difference between the implementation of 266 nm and 1064 nm prepulses. Similar CE was realized from both prepulse wavelengths, although the 266 nm prepulse require a 1 μs shorter delay to achieve this. The EUV spectral features were similar for both prepulse wavelengths. Ion TOF data showed that ionic debris from the 1064 nm prepulse was slightly less energetic than that from the 266 nm prepulse, but this difference is minor compared to the decrease in ion kinetic energies afforded by both prepulses when compared to kinetic energies produced by the individual pumping pulse.

ACKNOWLEDGEMENTS

This work is partially supported by SEMATECH Inc. and Purdue University.

REFERENCES

[1] Taylor, J. S., and Soufli, R., [Specification, Fabrication, Testing, and Mounting of EUVL Optical Substrates] SPIE and John Wiley & Sons, Inc., Bellingham, WA and Hoboken, NJ, 4C (2009).

[2] Bakshi, V., [EUV Source Technology: Challenges and Status] SPIE - The International Society for Optical Engineering, Bellingham, WA, 1 (2006).
[3] Banine, V. Y., Koshelev, K. N., and Swinkels, G. H. P. M., "Physical processes in EUV sources for microlithography," J. Phys. D Appl. Phys., 44(25), 253001 (2011).
[4] Harilal, S. S., Sizyuk, T., Hassanein, A., Campos, D. *et al.*, "The effect of excitation wavelength on dynamics of laser-produced Sn plasma," J. Appl. Phys., 109(6), 063306 (2011).
[5] Hassanein, A., Sizyuk, T., Sizyuk, V., and Harilal, S. S., "Combined effects of prepulsing and target geometry on efficient extreme ultraviolet production from laser produced plasma experiments and modeling," J. Micro/Nanolith. MEMS MOEMS, 10(3), 033002 (2011).
[6] Sizyuk, V., Hassanein, A., and Bakshi, V., "Modeling and optimization of debris mitigation systems for laser and discharge-produced plasma in extreme ultraviolet lithography devices," J. Micro/Nanolith. MEMS MOEMS, 6, 043003 (2007).
[7] White, J., Dunne, P., Hayden, P., O'Reilly, F. *et al.*, "Optimizing 13.5 nm laser-produced tin plasma emission as a function of laser wavelength," Appl. Phys. Lett., 90(18), 181502 (2007).
[8] Harilal, S. S., Sizyuk, T., Sizyuk, V., and Hassanein, A., "Efficient laser-produced plasma extreme ultraviolet sources using grooved Sn targets," Appl. Phys. Lett., 96(11), 111503 (2010).
[9] Nishihara, K., Sunahara, A., Sasaki, A., Fujioka, S. *et al.*, "Advanced laser-produced EUV light source for HVM with conversion efficiency of 5-7% and B-field mitigation of ions," Proc. SPIE. 6921, Y9210 (2008).
[10] Spitzer, R. C., Kauffman, R. L., Orzechowski, T., Phillion, D. W. *et al.*, "Soft x-ray production from laser produced plasmas for lithography applications," J. Vac. Sci. Technol. B, 11(6), 2986-2989 (1993).
[11] Tanaka, H., Matsumoto, A., Akinaga, K., Takahashi, A. *et al.*, "Comparative study on emission characteristics of extreme ultraviolet radiation from CO2 and Nd : YAG laser-produced tin plasmas," Appl. Phys. Lett., 87(4), 041503 (2005).
[12] Campos, D., Harilal, S. S., and Hassanein, A., "The effect of laser wavelength on emission and particle dynamics of Sn plasma," J. Appl. Phys., 108(11), 113305 (2010).
[13] Campos, D., Harilal, S. S., and Hassanein, A., "Laser wavelength effects on ionic and atomic emission from tin plasmas," Appl. Phys. Lett., 96(15), 151501 (2010).
[14] Takahashi, A., Nakamura, D., Tamaru, K., Akiyama, T. *et al.*, "Emission characteristics of debris from CO2 and Nd : YAG laser-produced tin plasmas for extreme ultraviolet lithography light source," Appl. Phys. B, 92(1), 73-77 (2008).
[15] Fujioka, S., Shimomura, M., Shimada, Y., Maeda, S. *et al.*, "Pure-tin microdroplets irradiated with double laser pulses for efficient and minimum-mass extreme-ultraviolet light source production," Appl. Phys. Lett., 92(24), 241502 (2008).
[16] Harilal, S. S., Tillack, M. S., Tao, Y., O'Shay, B. *et al.*, "Extreme-ultraviolet spectral purity and magnetic ion debris mitigation by use of low-density tin targets," Opt. Lett., 31(10), 1549-1551 (2006).
[17] Mizoguchi, H., Abe, T., Watanabe, Y., Ishihara, T. *et al.*, "1st generation Laser-Produced Plasma source system for HVM EUV lithography," Proc. SPIE. 7636, 763608 (2010).
[18] Fujioka, S., Nishimura, H., Okuno, T., Tao, Y. Z. *et al.*, "Properties of EUV and particle generations from laser-irradiated solid- and low-density tin targets," Proc. SPIE. 5751, 578-587 (2005).
[19] Coons, R. W., Harilal, S. S., Campos, D., and Hassanein, A., "Analysis of atomic and ion debris features of laser-produced Sn and Li plasmas," J. Appl. Phys., 108(6), 063306 (2010).
[20] Harilal, S. S., Coons, R. W., Hough, P., and Hassanein, A., "Influence of spot size on extreme ultraviolet efficiency of laser-produced Sn plasmas," Appl. Phys. Lett., 95(22), 221501 (2009).
[21] Higashiguchi, T., Kawasaki, K., Sasaki, W., and Kubodera, S., "Enhancement of extreme ultraviolet emission from a lithium plasma by use of dual laser pulses," Appl. Phys. Lett., 88(16), 161502 (2006).
[22] Anand, M., Kahaly, S., Kumar, G. R., Krishnamurthy, M. *et al.*, "Enhanced hard x-ray emission from microdroplet preplasma," Appl. Phys. Lett., 88(18), 181111 (2006).
[23] Freeman, J. R., Harilal, S. S., and Hassanein, A., "Enhancements of extreme ultraviolet emission using prepulsed Sn LPPs for advanced lithography applications," J. Appl. Phys., 110, 083303 (2011).
[24] Hurst, N., and Harilal, S. S., "Pulse shaping of transversely excited atmospheric CO2 laser using a simple plasma shutter," Rev. Sci. Instrum., 80(3), 035101 (2009).